ACS OMEGA

http://pubs.acs.org/journal/acsodf

Article

Pyrolysis of Sugarcane (*Saccharum officinarum* L.) Leaves and Characterization of Products

Mohit Kumar, Siddh Nath Upadhyay,* and P. K. Mishra

Cite This: *ACS Omega* 2022, 7, 28052−28064

Read Online

ACCESS | Metrics & More | Article Recommendations | Supporting Information

ABSTRACT: The finite nature, regional availability, and environmental problems associated with the use of fossil fuels have forced all countries of the world to look for renewable eco-friendly alternatives. Agricultural waste biomasses, generated through the cultivation of cereal and noncereal crops, are being considered renewable and viable alternatives to fossil fuels. In view of this, there has been a global spurt in research efforts for using abundantly available agricultural wastes as feedstocks for obtaining energy and value-added products through biochemical and thermal conversion routes. In the present work, the thermochemical characteristics and thermal degradation behavior of sugarcane leaves (SCL) and tops were studied. The batch pyrolysis was carried out in a fixed-bed tubular reactor to obtain biochar, bio-oil, and pyrolytic gas. Effects of bed height (4−16 cm), particle size (0.180−0.710 mm), heating rate (15−30 °C/min), and temperature (350−650 °C) were investigated. The maximum yields of bio-oil (44.7%), biogas (36.67%), and biochar (36.82%) were obtained at 550, 650, and 350 °C, respectively, for a 16 cm deep bed of particles of size 0.18−0.30 mm at the heating rate of 25 °C/min. The composition of bio-oil was analyzed using Fourier transform infrared spectroscopy (FTIR), proton nuclear magnetic resonance (^{1}H NMR), and gas chromatography−mass spectrometry (GC−MS) techniques. Several aliphatic, aromatic, phenolic, ketonic, and other acidic compounds were found in the bio-oil. The biochar had a highly porous structure and several micronutrients, making it useful as a soil conditioner. In the middle temperature ranges, biogas had more methane and CO and less hydrogen, but at higher temperatures, hydrogen was predominant.

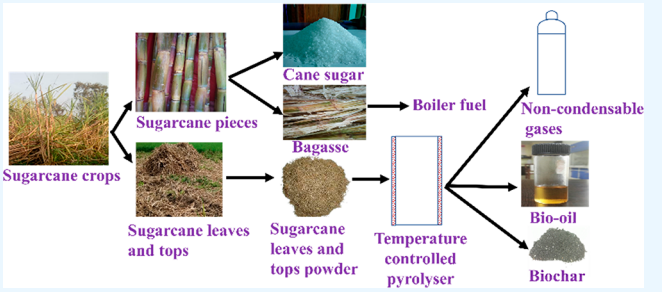

1. INTRODUCTION

Fossil fuels (petroleum crude, coal, and natural gas) have been responsible for the phenomenal development in practically all sectors of modern human society. The finite reserves and regional availability of these fuels and environmental issues such as acid rain, climate change, global warming, etc., resulting from their use have forced all countries to look for renewable and nonpolluting alternatives. The waste biomasses from agricultural, domestic, and industrial sectors are being considered eco-friendly renewable alternatives to fossil fuels. Over the past few decades, there has been an unprecedented growth in research and developmental efforts for generating scientific know-how for utilizing the abundantly available agricultural and nonagricultural waste biomasses as feedstock for producing energy and other value-added products through biochemical, chemical, and thermochemical routes. The lignocellulosic biomasses from cereal and industrial crops, etc. have the potential to replace fossil fuels in most sectors. As a result, global efforts are being made to use them as feedstock for obtaining clean energy and value-added products currently being obtained from petroleum and natural gas.[1]

India, a heavily and densely populated country, is highly dependent upon the import of crude petroleum. In 2013−2015, the Indian oil import amounted to 189.238 million metric tonnes of crude worth Rs 864, 875 crores. Thus, to ensure energy security and fulfill its global obligations of reducing the carbon footprint, India needs to focus heavily on renewable energy sources like biomass. Sugarcane (*Saccharum officinarum* L.), a perennial monocotyledonous plant of the Gramineae (Poaceae) family, is native to Asia but has now become one of the most important commercial crops in several tropical and subtropical countries. After Brazil, which accounts for one-fourth of the total global sugarcane produce, India is the second leading producer.[2] Figure 1 depicts the total land area utilized for sugarcane farming, peanut productivity globally, and average production in the top 10 nations from 1994 to 2019. In India, it is grown over an area of 4.95 million hectares, with a crop yield of 70.39 tonnes per hectare. Typically, sugarcane crop production results in about 25−30% of crop residues (sugarcane leaves and tops) as waste, making

Received: April 4, 2022
Accepted: July 14, 2022
Published: August 5, 2022

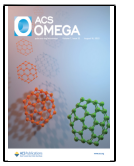

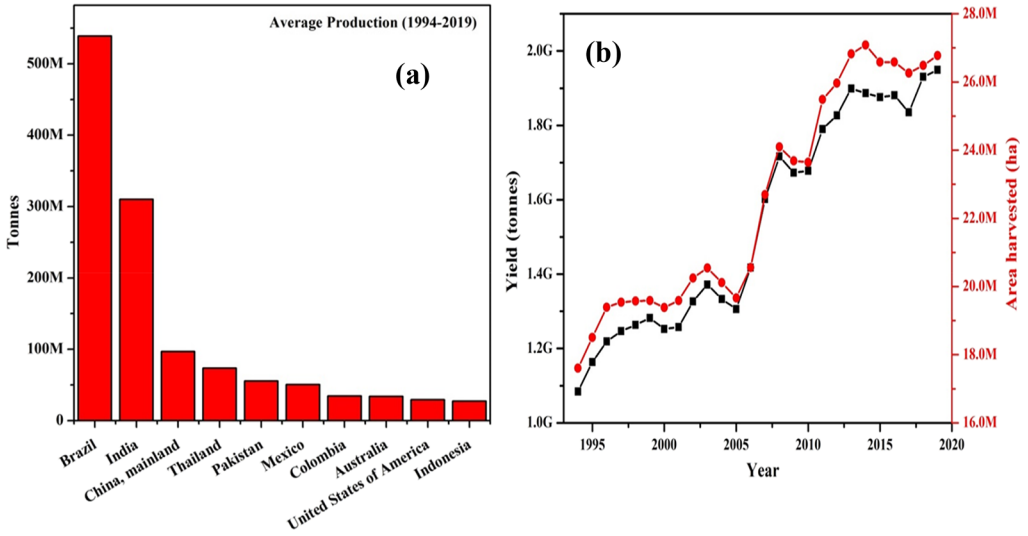

Figure 1. World production of sugarcane from 1994 to 2019: (a) production in top sugarcane-producing countries and (b) global cultivation area and yield.

it India's most abundant crop residue.[3,4] Currently, there is no proper management of this huge volume of residual biomass. Burning it in the field itself is the easiest method of its disposal, but this leads to the emission of CO, CO_2, NO_x, and particulate matter (fly ash) and reduces the diversity of soil microbes.[2]

The sugar cane trash (leaves and tops) and bagasse have a long history of use as a fuel in most cane-producing countries. Systematic studies for understanding the thermal degradation behavior (gasification, pyrolysis, torrefaction, etc.) for producing value-added products such as bio-oil, biochar, and biogas have attracted the attention of several researchers during the past 10 years. Tables 1 and 2 provide summaries of the published information that is currently available on the thermochemical properties of sugarcane trash and its thermal degradation behavior. The proximate and ultimate analyses and calorific values of leaves, tops, and bagasse have been determined by several workers. It has been shown that the storage time, particle size, and torrefaction have a profound effect on the fuel characteristics of sugar cane trash.[5,6] The bio-oil obtained through fast and slow pyrolysis of sugar cane bagasse and trash has been characterized, and it has been reported that bio-oil from bagasse has more phenols and that from leaves and trash has more hydrocarbons.[7] The bio-oil obtained from commercial pyrolysis units has been found to contain over 331 different molecules.[8] Jutakridsada et al.[9] reported four stages for thermal degradation of sugar cane leaves, whereas Chen et al.[10] reported only three stages. Rio et al.[11] observed differences in the structure and constituents of lignin from bagasse and sugar cane straw.

Charusiri and Numcharoenpinij[12] studied the effect of a catalyst (calcined dolomite) on the bio-oil yield and its constituents and observed lower oxygen-containing constituents in the product. Novais et al.[13] obtained improved biochar from $MgCl_2$-treated sugar cane straw capable of adsorbing phosphorus and having better soil conditioning capability.

Kinetic modeling of the thermal degradation process of sugar cane biomass (bagasse and trash) has been investigated by Chen et al.,[10] Rueda-Ordóñez and Tannous,[14] and Kumar et al.[15] using DAEM and iso-conversional models. Only a limited number of workers have tried to analyze the thermal degradation kinetics of sugar cane trash.

In India, sugar cane trash is used widely as fuel for making raw sugar ("gud") and jaggery using primitive furnaces and juice concentrating pans, but the scientific study of the combustion and thermal degradation behavior is scanty. Kumar et al.[4] were the first to study the thermal degradation kinetics and degradation mechanism of sugar cane trash using TG/DTG data. In the present work, the slow pyrolysis of sugar cane trash biomass in a fixed bed batch reactor has been carried out to maximize the yields of biochar, bio-oil, and gaseous products through the control of the operating parameters like bed height, biomass particle size, heating rate, and temperature on the yields for the first time. The results obtained are presented and discussed in this article.

2. EXPERIMENTAL SECTION

The sugarcane trash (leaves and tops), obtained from the sugarcane plantations of Kheri District (26.90°N 81.30°E) of U.P. (Uttar Pradesh) in India, was powdered after drying. The biomass powder thus obtained was used for thermochemical characterization, TG/DTG analyses, and batch pyrolysis in a fixed bed reactor to study the effects of various operating parameters (heating rate, temperature, bed height, and particle size). A schematic diagram of the steps followed is shown in Figure 2. The details of the specific procedures are discussed in the following sections.

2.1. Sugar Cane Biomass Collection and Sample Preparation. The SCL biomass samples were collected, cleaned in water, and allowed to dry for 3 days in the open air. After being divided into smaller pieces, the samples were dried for 24 h at 60 °C in a hot air oven (Universal Oven, Model, NSW143(OUA-2), New Delhi, India). The dried sample was powdered in a Wiley Mill (Model 2, Arthur H. Thomas Co, Philadelphia, USA) and sieved in a gyratory sieve shaker (Model: KI-133(a), Retsch, New Delhi, India) using sieves of the following sizes for 15 min to separate particles according to their size: >0.71, 0.710−0.425, 0.425−0.300, and 0.300−0.180 mm. The biomass of different sizes was used to study the effect of particle size on bio-oil, biochar, and biogas yields. Bulk densities (kg/m^3) of powder samples of different sizes were

https://doi.org/10.1021/acsomega.2c02076
ACS Omega 2022, 7, 28052−28064

Table 1. Summary of Reported Work on the Thermal Treatment of Sugar Cane Biomasses

references	process conditions	comments
8	analysis of bio-oil from a commercial installation; GC × GC/qMS analysis	Analysis indicated 331 constituents; 166 were confirmed by the linear-temperature-programmed reductive index (LTPRI)
16	sugar cane straw; D_p = 0.55 mm; fluidized bed reactor (id = 417 mm, height = 2600 mm); oxidative fast pyrolysis; T = 470, 550, and 600 °C; air flow = 85.6, 94.6, and 87.6 kg/h; feed rate of biomass = 147.30, 128.20, and 93.20 kg/h	The bio-oil had a reduced heating value of 22.95 MJ/kg, extremely little water content, and low oxygen content of 38.48 wt %. Because there were acid organic molecules present, the pH varied between 3.14 and 3.57. The yields of bio-oil and char reached up to 35.5 and 48.2 wt %, respectively. The amount of fixed carbon and volatile materials in the char was high. It had a 13.54 MJ/kg HHV value.
9	sugar cane leaves and corn stover; TGA analysis; T = 30−600 °C; HR = 10 °C/min	Thermal degradation involved four stages: dehydration, active pyrolysis, passive pyrolysis, and complete combustion. Sugar cane leaves had a higher ash content than corn stover. The heating values were obtained as 14.47 and 20.91 MJ/kg for sugarcane leaves and corn stover, respectively.
10	five ligno-cellulosic biomasses including sugar cane bagasse; D_p < 0.074 mm; mass = 5 mg; T = ambient to 800 °C; HR = 10 °C/min; N_2 flow = 120 mL/min	The pyrolysis of lignocellulosic biomass could be divided into three stages corresponding to the pyrolysis of hemicellulose, cellulose, and lignin, respectively. The single Gaussian E_α distributions for each stage range from 148.50 to 201.13 kJ/mol with 2.60 to 13.37 kJ/mol as the standard deviation. The three-parallel-DAEM model's initial estimate values were taken from the kinetic parameters of various phases.
11	sugar cane bagasse and leaves-lignin structures; Py/GC−MS unit; microfurnace pyrolizer, T = 500 °C	The lignin from straw had lower amounts of alkyl-aryl ether substructures and higher amounts of condensed structures such as phenylcoumarans and dibenzodioxocins than bagasse.
14	sugar cane straw; D_p = 510 μm; Shimadzu TGA unit; T = RT−900 °C; HR = 1.5, 2.5, 5,10, 15, 20, 40 °C/min; N_2 = 50 mL/min	The Friedman model was used to analyze the thermal degradation data. The two-dimensional diffusion described the reaction. The activation energy, E_α, ranged between 154.1 and 177.8 kJ/mol (average value = 149.7 kJ/mol) and A = 1.82 × 10^9/s.
17	sugar cane bagasse and straw; microwave irradiation of aqueous and acidic glycerol suspensions of biomass; incubated for 72 h at 55 °C; XRD, DTG, TGA, DSC, and TEM analysis	In sugarcane bagasse and straw fibers, microwave irradiation in combination with both aqueous and acid glycerol solutions caused minor physical changes. For the pretreated sample, TEM of the cell wall revealed certain areas of structural loosening, which increased the enzyme hydrolysis yield (1.4 times higher than untreated samples). Fibers were not harmed, and no inhibitors were released.
18	sugar cane residue; bench-top slow pyrolysis; T = 450, 550, 650, and 750 °C; HR = 20 °C/min; N_2 = 300 mL/min	Biochar generated at 650−750 °C has the greatest carbon content. Low H/C and O/C ratios, as well as pyrolysis fingerprints dominated by aromatic and polyaromatic hydrocarbon, are properties of biochars, which are often regarded as being stable in soil. These characteristics were evident in biochars generated at 550 °C.
19	sugar cane straw; fast pyrolysis; in a commercial plant (Petrobras, Brazil)	The characterization of organic extracts of bio-oil used GC−GC/TOFMS. Numerous oxygenated substances were discovered and categorized as acids, phenols, aldehydes, and ketones, with phenolic substances, primarily catechol, having a strong majority. Several alkylphenols (from C1 to C4 alkyl replacements) and alkyl benzenediols might be categorized (probably catechols, from C1 to C3 alkyl substitutes).
14	sugar cane straw; D_p = 0.25 mm; TGA; DSC; T = 30−900 °C; HR = 2.5, 5, 10 °C/min; synthetic air flow rate = 50 mL/min	The smoldering reaction was identified as consisting of three consecutive stages: drying, oxidative pyrolysis, and combustion. The Vyazovkin model was used for data analysis. The kinetic route consisted of six distinct parallel processes with activation energies of 176, 313, 150, 80, 150, and 100 kJ/mol, three for each step after drying. In synthetic air, the heat of reaction was entirely exothermic and released 8 MJ/kg. The thermal degradation of sugarcane straw was predicted, and the results showed good agreement with the data.
5	sugar cane trash; effect of particle size (<0.25, 0.25−0.420, and >0.420 mm); storage time: 0, 1, and 2 years	WDXRF and SEM results indicated variations in the results of the ash content with different particle sizes. Smaller particles (0.250 mm) were found to have a greater concentration of mineral contaminants. There was no statistically significant change in the HHV, which ranged from 15.9 to 18.3 MJ/kg. Its physicochemical properties are hindered by the particle size. The quality of the waste for use as a solid biofuel was unaffected and may be kept in the field.
3	sugar cane straw; D_p = 250−1000 μm; calcined dolomite as catalyst; SS316 tubular reactor; T = 400−600 °C; biomass feed rate = 0.3 to 1.2 kg/h; sweeping gas flow rate = 80−200 cm^3/min	The results showed that the SCS catalytic pyrolysis process produced liquid yields of 36.15 wt %, gas yields of 52.09 wt %, and solid yields of 11.76 wt % when using a pyrolysis temperature of 450 °C, 0.6 kg/h, 80 cm^3/min, and 500 m, respectively, with 10 wt % calcined dolomites. The calcined dolomite had an impact on the volatile vapor's carbonylation and cracking, which led to an improved bio-oil with less oxygen, a greater gross calorific value, and less acid corrosion.
7	sugar cane bagasse and straw; size: 30 mm; 3 g; fixed bed reactor, 27−700 °C; heating rate 100 °C/min; N_2 flow 100 mL/min; bio-oil analyzed using GC−MS	Bio-oil from bagasse had more phenols, and that from leaves had more hydrocarbons.
13	poultry manure, sugar cane straw; biomass + aq. $MgCl_2{\cdot}6H_2O$ (90 mL water +60 g salt) in a ratio of 1:10; T = 350 and 650 °C; HR = 10 °C/min	Biochar without Mg did not adsorb P. The poultry manure biochar exhibited a higher adsorption (250.8 and 163.6 mg P/g at 350 and 650 °C, respectively) than that of sugarcane straw (17.7 and 17.6 mg/g, respectively). Biochar can be used as slow P-release manure.
6	T = RT−250, 300, and 350 °C; HR = 10 °C/min; time = 0−75 min	The HHV of SCL increased to ∼22 MJ/kg after the torrefaction. The resulting SCL torrefied at 300 °C for 45 min was found to be suitable for industrial and domestic applications and has fuel ratio (FR), combustibility index (CI), volatile ignitability (VI), Hausner ratio (HR), and Carr compressibility index (CCI) within the prescribed values of 0.5−2.0, 12−23 MJ/kg, ≥14 MJ/kg, ≤1.34, and ≤25, respectively.
4	sugar cane leaves and top; D_p = 1 mm; TGA, DSC; T = 30−1000 °C; HR = 5, 10, 15, 20, 25, 40 °C/min; N_2 flow rate = 100 mL/min	Thermal degradation profiles were analyzed using Friedman, FWO, KAS, Tang, Starink, Vyazovkin, and Vyazovkin AIC models. The reaction mechanism was investigated using the Criado method; E_α = 214.9 to 239.6 kJ/mol.

https://doi.org/10.1021/acsomega.2c02076
ACS Omega 2022, 7, 28052−28064

Table 2. Thermochemical Properties of Sugar Cane Leaves (SCL) and Other Sugarcane-Based Residue Biomasses

analyses	present work	sugarcane straw[3]	sugarcane trash[5]	sugarcane straw[14]	sugarcane straw[16]	sugarcane leaves[23]	sugarcane bagasse[24]	sugarcane bagasse[25]	sugarcane bagasse[26]
Proximate analysis (wt %)									
moisture content	5.61	4.01		8.42 ± 0.30	10.40	5.44	7.41 ± 0.57	7.31	
volatile matter	77.33	73.41	77.22 ± 1.04	86.64 ± 0.53	74.00	72.13	80.98 ± 0.65	76.93	
ash content	6.38	2.38	4.63 ± 0.26	3.85 ± 0.21	16.40	10.26	4.09 ± 0.52	4.41	2.61
fixed carbon	10.67	18.20	18.14 ± 1.14	9.51 ± 0.53	13.00	13.13	7.52 ± 0.25	11.33	
VM/FC	7.25	4.03[a]	4.25[a]	9.11[a]	5.69[a]	5.49[a]	10.77 ± 2.6	6.79[a]	
Ultimate analysis (wt %)									
C	42.33	40.13		42.94 ± 0.25	43.20	42.70	46.19	46.95	39.97
H	5.81	7.72		6.26 ± 0.16	6.70	7.40	6.11	6.06	5.16
N	0.59	2.68		0.31 ± 0.05	0.30	0.45	0.59	0.13	0.18
O	51.57	36.65		46.65 ± 0.18	33.20	33.32	47.11	46.78	52.06
S					0.20			0.08	0.008
H/C	1.65						0.75	1.55	
O/C	0.91						1.58	0.74	
calorific value (MJ/kg)	18.08	17.83	18.10 ± 0.87	18.61	18.00	19.12	15.06		16.48

[a]Calculated values

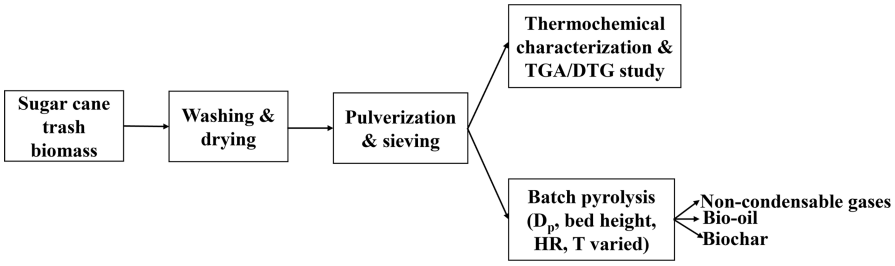

Figure 2. Sequence of experimental steps employed in this work.

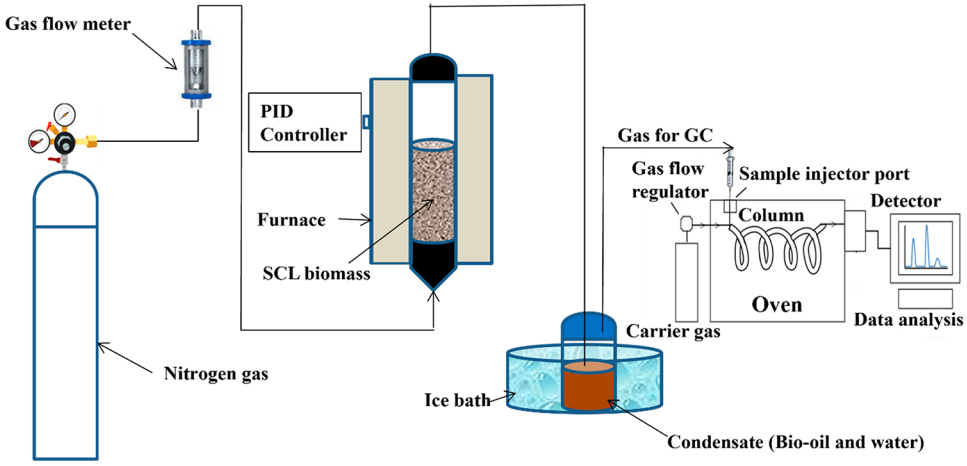

Figure 3. Simplified sketch of the pyrolysis setup.

measured using ASTM Standard Method-873. Biomass powder of size 0.18−0.30 mm was used for proximate and ultimate analyses, determination of HHV, and TG/DTG analyses.

2.2. Chemicals and Reagents. All chemicals used in the present work were of analytical grade. Dichloromethane, *N*,*N*-dimethyl formaldehyde, *n*-hexane, methanol, and deuterated dimethyl sulfoxide (DMSO) were obtained from Thermo Fisher Scientific, USA. The nitrogen gas (99% purity) was obtained from INOX AIR Products Ltd. in Greater Noida, India. The distilled water used for washing was prepared in the laboratory using a quartz double-distilled water still.

2.3. Thermochemical Characteristics of SCL Biomass. The proximate analysis of the biomass sample was carried out as per the ASTM protocols (E872-82 2006, E871-82 2006, and E1755-01 2007) to determine the moisture (MC), volatile matter (VM), and ash contents. All the experiments were performed in triplicate, and average values are presented. Fixed carbon (%) =100 − {MC (%) + VM (%) + ash content (%)} was the formula used to calculate the fixed carbon by difference. The elemental analysis (C, H, N, and S estimation) was carried out using a CHNS analyzer (Euro EA 3000, Elemental Analyzer, Lombardi a Milano, Italy). The difference was then used to calculate oxygen. Using a bomb calorimeter,

https://doi.org/10.1021/acsomega.2c02076
ACS Omega 2022, 7, 28052−28064

the sample's calorific value (MJ/kg) was calculated (Digital bomb Calorimeter, Model No. RSB 3, Rajdhani Scientific Inst. Co., New Delhi, India).

2.4. Thermogravimetric/Differential Thermogravimetric Analyses. With a heating rate of 15 °C/min, a Shimadzu thermogravimetric analyzer (TGA-50, 00377, Shimadzu Corp., Kyoto, Japan) was used to measure the thermal degradation of SCL in a nitrogen environment. The nitrogen flow rate was held constant throughout the TGA tests at 100 mL/min. With the aid of the program Origin Pro, the DTG data were produced using the TGA data. The TG/DTG-temperature profiles thus generated were used to evaluate the thermal degradation behavior with an increase in temperature and to find out the active pyrolysis zone where the maximum weight loss of the sample occurred. These results were used for deciding the temperature range for batch pyrolysis experiments.

2.5. Batch Pyrolysis Experiments. The laboratory-scale pyrolysis setup used in the present work is a packed bed batch pyrolyzer unit as shown in Figure 3. The pyrolysis unit is essentially a tubular reactor made of an SS tube of 520 mm length and 44 mm internal diameter mounted inside a vertical electrically heated tubular furnace equipped with a PID controller. An accurately weighed biomass powder sample (approximately 20 g) was taken for each run except in those runs that were used for investigating the effect of bed height. In the case of runs made for investigating the effect of bed height, different amounts of the biomass powder were taken to vary the biomass bed height. The bed height was evaluated indirectly by freely filling the known amount of powdered biomass in a glass tube of the same internal diameter as the SS tube. Throughout the experiments, nitrogen gas was kept flowing at a rate of 100 mL/min to provide an inert environment and serve as a carrier gas. Below the condenser, the condensable vapors were collected in a bottle submerged in an ice bath. After filling the biomass and starting the flow of nitrogen, the furnace was switched on. After reaching the desired temperature, the heating was kept on for an extra 30 min to ensure the complete accumulation of the entire condensable liquid product (aqueous bio-oil) and complete the biochar formation. The mass of aqueous bio-oil fraction and biochar residue was obtained by direct weighing of the liquid fraction collected in the flask and solid residue left in the reactor. The product yields (condensed liquid (aqueous bio-oil) and biochar) were estimated using the following equations:

$$\text{Bio} - \text{oil yield (wt\%)} = \frac{\text{bio} - \text{oil (g)}}{\text{biomass fed (g)}} \times 100 \quad (1)$$

$$\text{Bio} - \text{char yield (wt\%)} = \frac{\text{bio} - \text{char (g)}}{\text{biomass fed (g)}} \times 100 \quad (2)$$

The gas yield was calculated from the difference relation

$$\text{Gas yield (wt\%)} = 100 - \{\text{bio} - \text{oil yield (wt\%)} + \text{bio} - \text{char yield (wt\%)}\} \quad (3)$$

and the conversion was calculated using the relation

$$\text{Conversion (\%)} = 100 - \{\text{bio} - \text{char yield (wt\%)}\} \quad (4)$$

2.6. Characterization of Pyrolysis Products. The proximate and ultimate analyses of the biochar and bio-oil (only ultimate analysis) were carried out according to the ASTM standards used for raw biomass powder. The higher heating values (HHV, MJ/kg) of the bio-oil and biochar were evaluated using a digital bomb calorimeter (Digital Bomb Calorimeter, Model No. RSB 3, Rajdhani Scientific Inst. Co., New Delhi, India). The fuel characteristics of bio-oil (acidity, ash content, pH, Ramsbottom carbon residue, density, kinematic viscosity, and moisture content) were determined as per the API protocols.[20] The FTIR spectroscopic analyses were carried out by performing FTIR spectrometer analysis (FTIR 5700, Thermo-Electron Corporation, Massachusetts, USA) to confirm the functional groups of chemical compounds in raw biomass and pyrolysis products. The ^{1}H NMR spectroscopic analysis of the bio-oil was examined using a high-resolution ^{1}H NMR spectrometer ((Bruker BioSpin International AG, Model: AVH D 500 AVANCE III HD 500 MHz One Bay NMR Spectrometer). The solvent for the NMR analysis was deuterated DMSO (dimethyl sulfoxide). The molecular composition of the bio-oil was analyzed using a gas chromatography−mass spectrometry unit (Shimadzu-QP201, Kyoto, Japan) available in the department to know the constituent compounds.

The composition of the stable gaseous product of pyrolysis was determined using a gas chromatograph (GC-TCD Centurion Scientific, Model Number 5800, New Delhi) equipped with flame ionization (FID) and thermal conductivity (TCD) detectors that were coupled with a PORAPAK-Q filled SS column (length = 2 m, diameter = 2 mm). Nitrogen (flow rate = 25 mL/min) was used as the carrier gas. The injector and detector temperatures for the TCD were maintained at 110 and 120 °C, respectively, and those for the FID were maintained at 70 and 80 °C, respectively. A Hamilton Bonaduz (Switzerland) gas-tight syringe (0.1 mL) was used to inject the gas mixture for analysis.

3. RESULTS AND DISCUSSION

3.1. Particle Size Distribution and Bulk Density. The size of particles present in the biomass sample being pyrolyzed is an important parameter as it controls the heat and mass transfer processes affecting the thermal conversion. Less time is needed for the thermal conversion of small particles.[21] The biochar yield reduces, but the gas and bio-oil yields increase.[22] Smaller particles permit the improved transfer of heat and greater thermal conversion. In this work, in all the characterization experiments, particles of size 0.180−0.300 mm were used. As expected, the bulk density increased with decreasing particle size in the order 0.710 < 0.710−0.425 < 0.425−0.300 < 0.300−0.180 <0.180 mm (Figure S1). The process of pyrolysis and thermal decomposition of a feedstock material is affected by the particle size and hence also by the bulk density.

3.2. Thermochemical Properties of Biomass. The proximate and ultimate analyses results and HHV of sugar cane trash (leaves and tops) and bagasse reported by various workers are listed in Table 2. From this table, it is seen that moisture content has varied from 4.01 to 10.40%, VM from 72.13 to 86.64%, FC from 7.52 to 18.20%, and ash content from 2.38 to 18.20%. The carbon, hydrogen, and oxygen contents have varied from 39.97 to 46.95, 5.16 to 7.7, and 32.2 to 52.06%. The nitrogen content in bagasse and cane trash has varied in the range of 0.13 to 0.59%, except in one case where it is reported as 2.68%. A low amount of sulfur has been reported by three researchers. The HHV has ranged from

https://doi.org/10.1021/acsomega.2c02076
ACS Omega 2022, 7, 28052−28064

15.06 to 18.61 MJ/kg; the values for bagasse are the lowest. The low nitrogen and sulfur contents and high VM content and HHV clearly indicate that sugarcane-derived biomass is a good renewable fuel.

3.3. Thermogravimetric Analysis. The TG/DTG analyses of SCL powder were performed only at the heating rate of 15 °C/min in the temperature range of ambient to 800 °C. The TG and DTG degradation profiles are shown in Figure 3 as residual percent weight (%) and percent weight change rate (% change/min) versus temperature (°C) plots. The weight (%) versus temperature profile displays three distinct stages of thermal degradation (weight loss). Stage I is from room temperature to 260 °C, stage II is from 260 to 550 °C, and stage III is from 550 to 800 °C. In stage I, the observed weight loss is low (8%) due to the removal of moisture content (exterior and trapped moisture in the intercellular space) and some extremely volatile components of biomass.[4] The high weight loss (66%) observed in stage II is mainly because of the thermal cracking of hemicellulose and cellulose components of biomass. The complex low volatile organic compounds are formed and released slowly from the lignocellulosic biomass in stage III.[23] Therefore, the thermal degradation in this stage is prolonged, and the weight loss (3.3%) is very low compared to stage II. At the end of stage III, the residual mass becomes nearly constant (at around 22.7%), suggesting the completion of the conversion of biomass into biochar. This stage is often known as the char formation stage.[4]

The DTG analysis data were obtained by differentiating the TGA data and are shown as a function of temperature in Figure 4. The DTG profile exhibits three peaks. The first peak,

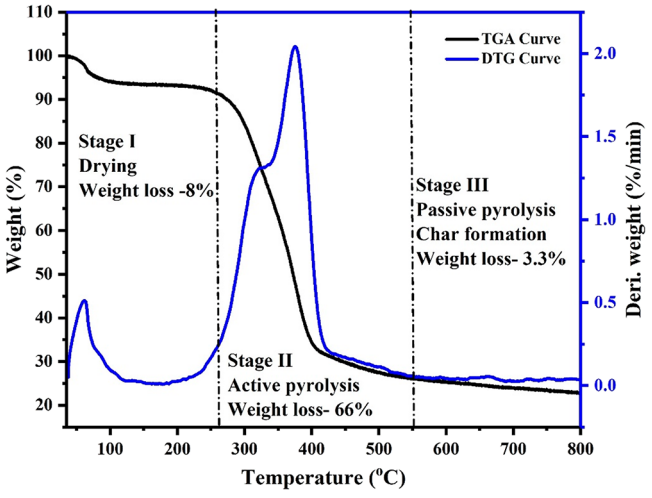

Figure 4. The TGA and DTG profile of SCL pyrolysis.

observed in stage I at around 60 °C, is due to the removal of moisture and highly volatile organic compounds at a rate of 0.5%/min. From 120 to around 200 °C, practically no change in residual weight % is observed, indicating the completion of the removal of moisture and highly volatile organic molecules. The second and third peaks observed in stage II are due to hemicellulose and cellulose degradation. The hemicellulose degradation peak is observed at 321 °C at the rate of 1.3%/min, and the cellulose degradation peak is observed at 374 °C at the rate of 2.03%/min. After around 425 °C, the observed residual biomass is primarily due to char formation within the extremely slow release of degradation products (0.058%/min).

3.4. Batch Pyrolysis Experiments. The batch pyrolysis experiments were performed in the active pyrolysis zone (stage II) at 350, 450, 550, and 650 °C (stage III) by varying the heating rate (15, 20, 25, and 30 °C/min) and biomass bed height (4, 8, 12, and 16 cm) and particle size (>0.71, 0.71−0.429, 0.429−0.30, and 0.30−0.18 mm). The results obtained are summarized in Table 3 and shown in Figure 5.

3.4.1. Effect of Process Temperature. Variations in the yields of gaseous, liquid, and solid products with temperature were investigated at 350, 450, 550, and 650 °C using biomass particles of 0.180−0.300 mm size and a bed height of 16 cm at the heating rate of 25 °C/min. As the temperature increased, the conversion of biomass into end-products also increased. Charusiri and Vitidsant[3] reported a similar effect on temperature. The yield of gaseous products increased from 26.27% at 350 °C to 36.20% at 650 °C. This can be attributed to the rapid thermal degradation of biomass into more noncondensable gases at a higher temperature due to secondary degradation reactions.[3]

The yield of liquid product (bio-oil) increased up to 550 °C, and thereafter, it decreased due to the formation of noncondensable products through the continuous cracking of the intermediate organic molecules produced through the primary and secondary reactions into gaseous products (Figure 4a). The solid product (biochar) decreased with an increase in temperature (Figure 4a). This may be attributed to the higher decomposition efficiency (higher heat and mass transfer among biomass particles) and the secondary conversion of char into noncondensable gas.[27]

3.4.2. Effect of Heating Rate. The variations in the yields of pyrolytic products with the heating rates (15, 20, 25, and 30 °C/min) are depicted in Figure 4b. The yield of bio-oil increased from 34.25% at 15 °C/min to 44.23% at 25 °C/min and then decreased to 34.12% at 30 °C/min. Similar trends were reported by Mishra and Mohanty[27] for neem seeds and by Xiong et al.[28] for rice husks. It was also observed that the liquid yield was higher than the biochar and gas yields at all heating rates except at 30 °C/min. Thus, it can be concluded that the pyrolysis of sugar cane trash biomass at low and medium heating rates results in an increased yield of bio-oil but decreased yield of biochar. This decrease could be either due to the higher primary decomposition of biomass leading to gaseous and condensable products or due to the secondary decomposition of the biochar.

The noncondensable gas yields increased as the temperature increased for medium and high heating rates. At high heating rates, the condensable thermal degradation products would be heated quickly to a high temperature, causing the formation of a large amount of noncondensable products through cracking.

3.4.3. Effect of Particle Size. Biomass particle size affects the heat and mass transfer processes affecting the thermal degradation of biomass, volatilization to lower molecular size constituents, and thermal decomposition of oily products (tar) during pyrolysis. The variation in yields of pyrolytic products obtained through the pyrolysis of SCL particles of sizes >0.71, 0.710−0.425, 0.425−0.300, and 0.300−0.180 mm at 550 °C is depicted in Figure 4c. It is seen that the yield of bio-oil has decreased slightly with the rise in the particle size due to inadequate heat and mass transfer, consequently resulting in the incomplete pyrolysis of biomass sample.[27] The yield of gaseous products is independent of particle size. During pyrolysis, adequate heat transfer to smaller biomass particles with a higher heating rate facilitates the decomposition of

https://doi.org/10.1021/acsomega.2c02076
ACS Omega 2022, 7, 28052−28064

Table 3. Sugar Cane Trash Biomass Pyrolysis: Product Distribution

				pyrolysis product (wt %) and conversion (%)			
temperature (°C)	heating rate	bed height (cm)	particle size (mm)	bio-oil	biochar	gas	conversion
350	25	16	0.300−0.180	36.71	36.82	26.47	63.18
450	25	16	0.300−0.180	41.82	30.64	27.54	69.63
550	25	16	0.300−0.180	43.78	25.02	31.20	74.98
650	25	16	0.300−0.180	39.28	24.05	36.67	75.95
550	15	16	0.300−0.180	34.71	33.82	31.47	66.18
550	20	16	0.300−0.180	42.82	29.64	27.54	70.36
550	25	16	0.300−0.180	44.78	26.02	29.20	73.98
550	30	16	0.300−0.180	37.28	23.05	39.67	76.95
550	25	4	0.300−0.180	34.71	31.62	33.67	68.38
550	25	8	0.300−0.180	37.69	30.14	32.17	69.86
550	25	12	0.300−0.180	40.38	27.32	32.30	72.68
550	25	16	0.300−0.180	42.18	24.15	33.67	75.85
550	25	16	0.300−0.180	41.23	32.16	26.61	67.84
550	25	16	0.425−0.300	39.62	35.63	24.75	64.37
550	25	16	0.710−0.420	38.69	34.26	27.05	65.74
550	25	16	>0.71	37.95	35.12	26.93	64.88

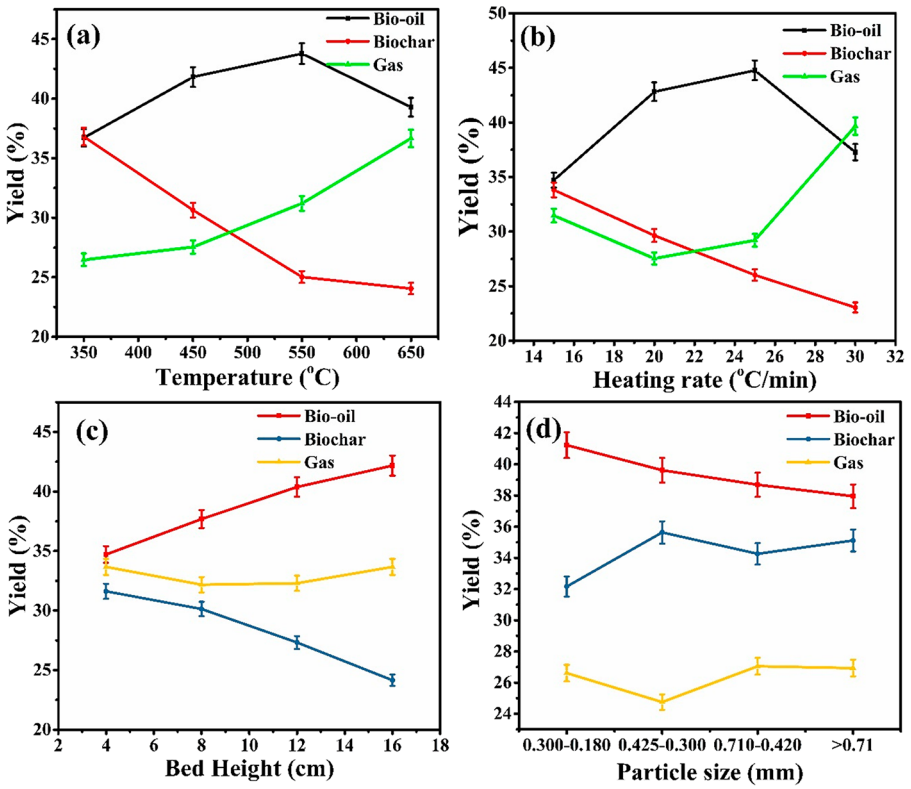

Figure 5. Effect of process parameters (a) temperature, (b) heating rate, (c) packed bed height, and (d) particle size on product yields.

biomass components into volatile vapors that create more noncondensable gases and, therefore, less biochar.

As the particle size increases, the pyrolysis process of biomass occurs primarily on the surface. The size distribution of the particle and the uniform nature of the biomass particles influence the heat and mass transfer processes. The resistance to heat transfer affects the liquid products more intensely on an increase in the average particle size as the internal temperature during the primary pyrolysis stage is insufficient for completing the thermal degradation process.[1,29−31]

3.4.4. Effect of Bed Height. It can be inferred from Figure 4d that the bio-oil yield has shown a gradual increase, but the yields of gaseous products and biochar have shown a marginal decrease with an increase in the bed height in the reactor from 4 to 16 cm. This behavior can be attributed to the increased residence time of degradation products within the pyrolysis zone leading to more secondary cracking reactions. Similar effects of bed height on biochar and gaseous products yields were reported by Gupta and Mondal[32] for sawdust and by Zhang et al.[33] for corncob.

3.5. Characterization of Bio-oil. *3.5.1. Physicochemical Properties of Bio-oil.* The condensable products of pyrolysis of biomass (bio-oil) comprise an aqueous phase (soluble organics dissolved in water) and organic phase. The collected liquid

https://doi.org/10.1021/acsomega.2c02076
ACS Omega 2022, 7, 28052−28064

product from the bottom of the condensing unit was treated with dichloromethane (CH_2Cl_2) to separate the organic phase from the aqueous.[23] The physicochemical properties of bio-oils (organic phase) produced during the pyrolysis of SCL at the optimum conditions (temperature: 550 °C, heating rate: 25 °C/min, bed height: 16 cm, and particle size: 0.300-0.180 mm) are presented in Table 4 together with the relevant properties

Table 4. Physicochemical Properties of the Sugar Cane Biomass Derived Bio-oil Compared with Petroleum Diesel Oil

properties	bio-oil	diesel
ultimate analysis (wt %):		
C	52.23	86.50
H	8.29	13.20
N	0.56	0.00
O	38.92	0.00
S		0.30
H/C	1.90	1.83
O/C	0.55	0.00
N/C	0.009	0.00
empirical formula	$CH_{1.90}O_{0.55}N_{0.009}$	$CH_{1.83}S_{0.0013}$
appearance	dark brown	
moisture content (wt %)	~8.26	0.00
pH	2.12	
acidity (mg_{KOH}/g)	28	
density (kg/m^3)	1089	820
kinetic viscosity (Pa·s)	0.69	
Ramsbottom carbon residue (wt %)	2.89	
HHV (MJ/kg)	27.39	
ash content (wt %)	0.06	0.00

of commercial diesel. Approximately 8 wt % moisture is there in the bio-oil, which is lower than the moisture content in bio-oils obtained from other biomasses including sugarcane (from 15 to 30%).[23,34] The elemental analysis of bio-oil revealed that its carbon content, H/C, and O/C are smaller than those for the raw SC biomass. This is due to the conversion of several carbons bearing low molecular weight organics as non-condensable products and the formation of CO and CO_2.[23]

The bio-oil was found to be acidic in nature, having a pH of 2.12, due to the presence of carboxylic acids, phenolic compounds, and their derivatives that make it corrosive.[17] The acid number estimated by the titration method using *N*,*N*-dimethyl formaldehyde and methanol as the solvent has been found to be 28 mg KOH/g, which is in close agreement with the published results.[23] The density of bio-oil (1089 kg/m^3) is more than that of diesel due to the presence of oxygenated organic compounds such as phenols.[32,35] The Ramsbottom carbon residue (RCR) is 2.89 wt %, and the ash content is 0.06 wt %. The higher heating value is 27.39 MJ/kg, indicating its good fuel property. These properties together with the empirical formula are reported in Table 3 and are in agreement with the published data.[35]

3.5.2. FTIR Spectroscopic Analysis of Bio-oil. The FTIR spectra of the bio-oil are depicted in Figure S2. The broader peak in the range of 3400 and 3500 cm^{-1} is due to the hydroxyl (O−H) group of phenolic and alcoholic compounds.[36] The peak at around 3000 cm^{-1} is dedicated to the C−H stretching of alkanes and alkenes present in the bio-oil.[37] Peaks noted between the 1600 and 1500 cm^{-1} wave number range represent the −CHO group of an aldehyde, −CO− group of a ketone, and $-CO_2H$ group of a carboxylic acid.[38] Numbers of small peaks observed between 1000 and 1500 cm^{-1} are due to the C−O stretching of ethers and esters.[1,33] The C−H vibrations of alkenes are in the range of 610−620 cm^{-1}.[39] Therefore, it may be concluded that the bio-oil is a mixture of valuable organic compounds that may be used as liquid fuel after upgrading or as a source of useful chemicals and fuel. The detailed information on the organic constituents of bio-oil was obtained using GC−MS analysis and is discussed in the following section.

3.5.3. GCMS Analysis of Bio-oil. The GC−MS analysis of the bio-oil fraction was carried out to identify the organic components present in the sample. For this purpose, the bio-oil sample was first diluted with hexane and then analyzed. The chromatograph indicated more than 100 peaks, and the corresponding components were identified with help of the National Institute of Standards and Technology (NIST) library. The major identified compounds are presented in Table 5.

The leaves and stalk of sugar cane are covered with a thin whitish to dark-yellowish powdery deposit of a waxy material that appears as a cuticle layer over the matrix of cellulose, hemicellulose, and lignin. Depending upon the variant of the sugar cane, the amount of waxy cuticle ranges from 0.1 to 0.3%.[40] Besides these simple phytosterols, ketosteroids, hydroxy-ketosteroids, and higher terpenoids are also present in it.[40] Thus, the bio-oil obtained through the pyrolysis of sugar cane leaf and top powder will be a complex mixture of all these together with their degradation products as well those of the cellulose, hemicellulose, lignin and other secondary products formed through their interaction.

The results of GC−MS analysis support the inferences drawn from the FTIR spectra. Aromatics like benzene, phenols, and their derivatives were obtained through the thermal degradation of cellulose, hemicellulose, and lignin present in the biomass. The major phenolic and other compounds include phenol, 2,6-dimethoxy-, decane, creosol, phenol 4-ethyl-2-methoxy-, 2-furanmethanol, 2-cyclopentene-1-one, 2-cyclopenten-1-one, 2-methyl-, phenol, 4-(2-propenyl)-2,6-dimethoxy-, 3-methylcyclopentane-1,2-dione, 3-methyl-, 2-methyl-3-hexanone, 2-cyclopentene-1-one, 3-ethyl-2-hydroxy-, (*E*)-9-octadecenoic acid ethyl ester, phenol, 2,6-dimethoxy-, 5-methyl-1,3-benzenediol, phenol, 2-methoxy-4-(1-propenyl)-, and 2-propanone, ethyl 9-hexadecenoate and are due to the decomposition of various compounds present in the waxy cuticle.[40] Acidic compounds and their derivative, such as acetic acid, butanoic (or butyric) acid, etc., are formed mainly due to the decomposition of hemicelluloses.[41] The nitrogenous compounds like pyridine, 2-ethyl-, *N*-(*n*-butoxymethyl) acryl-amide, pyridine2, 5-dimethyl-, etc., may be attributed to the heterocyclic ring containing compounds present in the biomass.

3.5.4. ^1H NMR Analysis of Bio-oil. The ^1H NMR spectroscopic analysis is an essential technique to get an idea and to gain a deeper understanding of the constituents and properties of thermally produced bio-oils.[41,42] The integral values of the specific peaks are presented in Table 6. The protons of the nonaromatic hydrocarbon and alkyl group carrying molecules are indicated by the unfilled area of ^1H NMR (0.5 to 1.5 ppm) spectra. The protons of the allylic groups found in carbonyl group, olefin, aromatics, and amides correspond to the next region (1.8 to 2.8 ppm). The spectra for 2.8 to 4.5 ppm refer to protons in alcohol, ether, and ester-

https://doi.org/10.1021/acsomega.2c02076
ACS Omega 2022, 7, 28052−28064

Table 5. Results of GC−MS Analysis of Sugar Cane Biomass Bio-oil

r. time	area %	name
6.448	7.89	2-furanmethanol
6.521	9.56	phenol, 2,6-dimethoxy
6.628	3.32	2-(acetyloxy)ethyl acetate
6.990	0.32	1,6,6-trideuterocyclohexa-2-EN-1-OL
7.260	2.15	2-cyclopenten-1-one, 2-methyl-
7.393	1.11	ethanone, 1-(2-furanyl)-
7.498	0.61	silane, phenyl-
7.864	1.70	*N*-(*n*-butoxymethyl) acrylamide
7.882	3.02	benzene, 1,2,4,5-tetrafluoro-3-methoxy-
8.675	5.24	phenol, 4-(2-propenyl)-2,6-dimethoxy-
9.308	0.27	2(5H)-furanone, 3-methyl-
9.500	0.16	decane
9.628	0.28	2-furan methanol, acetate
9.923	2.62	3,5-dimethoxy-4-hydroxyphenylacetic acid
10.871	3.92	3-methylcyclopentane-1,2-dione
11.258	0.27	oxazole, 2-ethyl-4,5-dihydro-
11.960	1.70	2-furaldehyde diethyl acetal
12.158	0.48	2-octen-4-ol
12.514	10.56	phenol, 2-methoxy-
13.340	0.25	octanoic acid, methyl ester
14.258	0.10	bicyclo heptane-1,2-dicarboxylic acid
14.361	0.23	2-pentanone, 5,5-diethoxy-
14.863	0.29	4,4,6-trimethyl-cyclohex-2-en-1-ol
15.178	0.29	phenol, 3-ethyl-
15.497	1.45	creosol
17.872	1.12	phenol, 4-ethyl-2-methoxy-
19.916	0.72	phenol, 2,6-dimethoxy-
21.000	0.12	decanoic acid, ethyl ester
23.218	0.22	benzene, 1-(1,5-dimethyl-4-hexenyl)-4-methyl-
26.050	0.17	hexadecane
30.353	0.19	ethyl 2-hydroxy-4-methoxy-6-propylbenzoate
33.041	0.17	hexadecanoic acid, methyl ester
36.524	0.45	9,12-octadecadienoic acid, methyl ester
37.456	3.06	linoleic acid ethyl ester
37.540	6.74	(*E*)-9-octadecenoic acid ethyl ester
37.857	0.99	octadecanoic acid, ethyl ester
38.512	0.30	methyl 9-cis,11-trans-octadecadienoate
38.642	0.57	cyclopropaneoctanoic acid, 2-hexyl-, methyl ester
38.929	0.19	3,5-dimethoxy-4-hydroxycinnamaldehyde
39.489	1.58	ethyl 9-hexadecenoate
40.709	0.26	1,2-benzenedicarboxylic acid
40.817	0.23	octadec-9-enoic acid
41.575	0.21	9-octadecenoic acid (*Z*)-, 2-hydroxy-1 (hydroxymethyl) ethyl ester
41.783	0.43	phenol, 2-methoxy-
42.833	0.18	heptadecanoic acid, ethyl ester

Table 6. Results of ^{1}H NMR Analysis of Bio-oil

chemical shift (ppm)	type of hydrogen present
0.5−1.5	proton present in the short-chain aliphatic group and many molecules with nonfunctional alkyl portions will give a lot of signals in this area
1.8−2.8	proton on the allylic group and appears when carbonyl group, olefin, or aromatics of the double-bond functional groups are present
2.8−4.5	proton present for alcohol, ethers of ester functional group that contains a single oxygen bond and CH_2 with two aromatic rings
6.5−8.5	protons of aldehyde functionality

containing single bonds of oxygen and CH_2 bound to two aromatic rings. The peaks in the 6.5 to 8.5 ppm region correspond to the aldehyde group protons.

3.6. Biochar Characterization. Physicochemical properties (proximate, ultimate, and higher heating values) of biochar are presented in Table 7. It is seen that the moisture content of biochar is lower than that of the raw biomass. The volatile matter (VM) of biochar is 10.45%, and the fixed carbon is 10.96%. The increment of ash content in biochar is because of the removal of volatile matter present in raw biomass and the collection of inorganic elements.[43] The ash content in the biochar is lower than that in the Indian coal (25 to 40%).[44] Compared to the virgin biomass, the VM/FC ratio of biochar is lower (0.13) and HHV is higher (23.46 MJ/kg) due to the higher fixed carbon content, indicating its better fuel quality. The H/C ratio is less than 1.0 due to increased carbonization.

Table 7. Physicochemical Properties of Biochar Obtained from Sugar Cane Trash

analysis		ICP AES analysis	
proximate analysis (wt %)		sodium	3.01
moisture content	1.12	magnesium	5.19
volatile matter	10.45	aluminum	4.56
ash content	10.96	silica	8.37
fixed carbon	78.59	potassium	5.63
VM/FC	0.13	calcium	10.23
ultimate analysis (wt %)		manganese	3.13
C	78.35	BET surface area (m^2/g)	235.17
H	5.14		
N	0.37		
S			
O	16.14		
H/C	0.79		
O/C	0.15		
HHV (MJ/kg)	23.46		

3.6.1. XRD Analysis of Biochar. The X-ray diffraction patterns of biochar and virgin biomass powder are shown in Figure 6. At 2Φ values of about 18.5 and 22.5°, the intensity and sharpness of the peaks indicate the amorphous and crystalline cellulose in virgin biomass. The peaks for biochar are reduced due to pyrolysis, suggesting cellulose degradation.[45] The peaks observed in Figure 5 from 25 to 30° correspond to the structure of crystallography. Other investigators have also confirmed the presence of such a

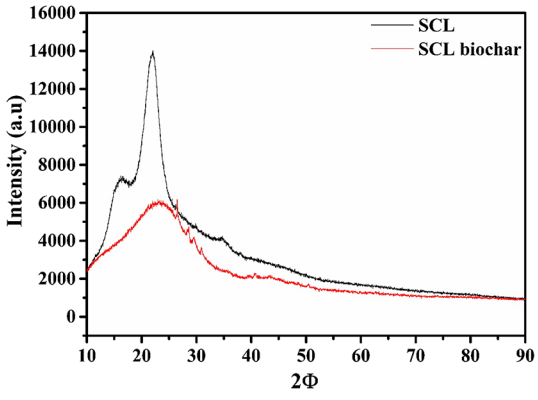

Figure 6. X-ray diffractogram of SCL biochar and SCL.

https://doi.org/10.1021/acsomega.2c02076
ACS Omega 2022, 7, 28052−28064

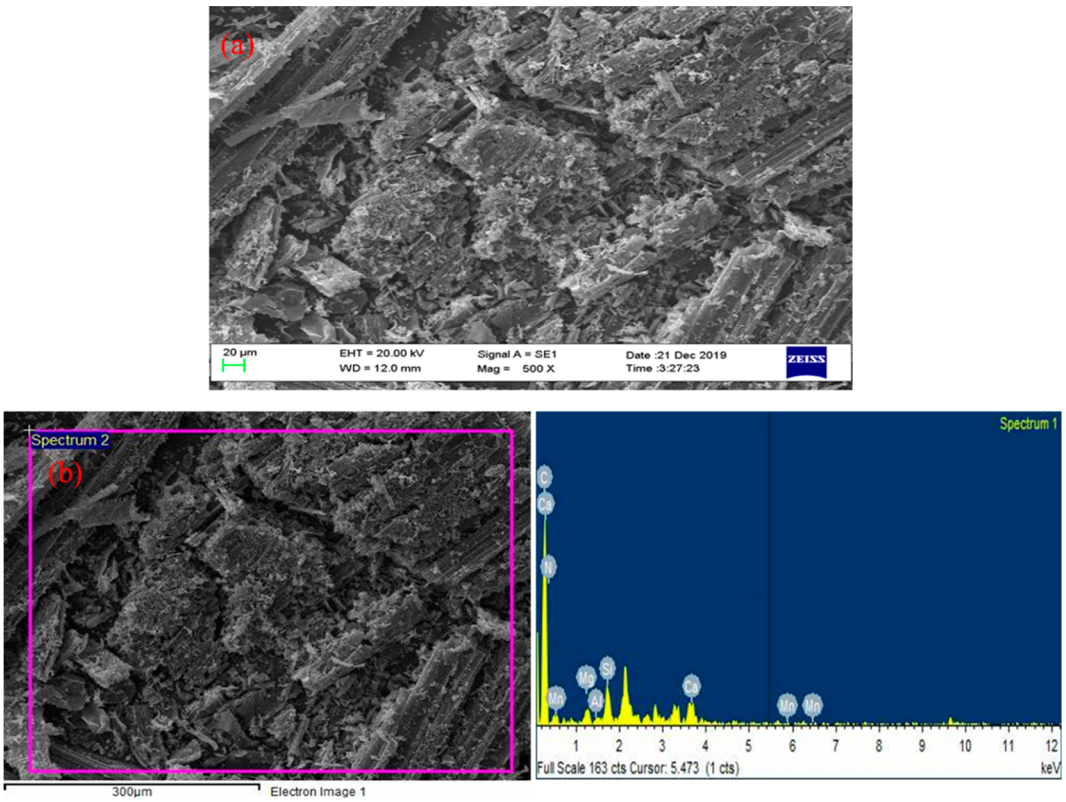

Figure 7. (a) FESEM image of biochar and (b) EDX spectra of biochar.

peak.[46] The peak at around 2Φ = 30° corresponds to the structure of calcite.[46] The rise in the intensity of the peak indicates the proportional decrease in the amorphous organic matter and rise in the ash content, as well as the structural transformation in the SCL biochar.[47]

3.6.2. SEM and EDX Analyses of Biochar. The SEM photo micrograph of SCL biochar is shown in Figure 7a,b. This picture shows a large number of pores and cracks on the surface of char particles. The EDX spectra of biochar shown in Figure 7b indicate the presence of N, C, Mn, Ca, Si, Al, and Mg.

3.6.3. ICP-AES Analysis of Biochar. The results of ICP spectroscopic analysis of biochar are given in Table 7. It is seen that the metallic elements like Al, Ca, K, Mg, Mn, Na, and Si are abundant in the biochar. Nitrogen, potassium, and phosphorus (Table 7) are the most common elements in the biochar, making it suitable as a soil conditioner.

3.6.4. FTIR Spectra of Biochar. The FTIR spectra of biochar in the wavenumber range of 500 to 4000 cm^{-1} are presented in Figure S2. The wide band in the wavenumber range of 3600-3200 cm^{-1} is assigned to the O−H groups of moisture and alcoholic and phenolic compounds.[48] The peak at 2900 cm^{-1} is due to the stretching of aliphatic C−H.[49] The peaks in the range of 2300−2000 cm^{-1} are attributed to the presence of carboxyl groups.[50] The lower sharp peak observed at around 1590 cm^{-1} is attributed to the C═C stretching and the presence of alkenes and aromatics. The peaks at approximately 1200 cm^{-1} agree with the C−H bending vibration, suggesting the presence of alkanes.[50] The stretching vibrations of aromatic C−H are indicated by the weak peak in the range of 1000−700 cm^{-1} and reflect the appearance of aromatic hydrogen.[51]

3.6.5. Thermal Stability of Biochar. The thermogravimetric and differential thermogravimetric analyses (TGA/DTGA) were carried out at the heating rate of 15 °C/min to study the thermal stability of biochar produced during the pyrolysis of SCL (Figure S3). It is seen that, up to 150 °C, approximately 10% weight loss occurs at the rate of 0.7%/min. This is due to the adsorbed moisture from the environment. After 150 °C, there is hardly any weight loss up to 450 °C, whereas in case of the raw SCL, mass loss continued up to 450 °C. The highest weight loss rate is observed at about 575 °C. The observed mass loss in the range of 450 to 625 °C is mainly due to the degradation of residual hemicellulose, cellulose, and lignin present in biochar, and a similar behavior has been reported by Mazlan et al.[51] for biochar obtained from Meranti wood sawdust (MWS) and by Salgado et al.[52] for Babassu endocarp biochar.

3.7. Gaseous Products. The variation in the composition of gaseous products of pyrolysis at different temperatures (300 to 600 °C) is shown in Figure 8. The gaseous product of pyrolysis contained hydrogen (H_2), methane (CH_4), carbon monoxide (CO), and carbon dioxide (CO_2). At lower temperatures (up to 415 °C), amounts of CO and CO_2 were found to be higher than hydrogen and methane. This can be attributed to the combustion of oxygen bearing constituents (cellulose and hemicellulose) of the biomass that are fully degraded up to 500 °C.[53] Other compounds responsible for CO_2 release are the C═O and −COOH group containing species in the virgin biomass, and at higher temperatures, it may be due to the decomposition of lignin.[54] The concentration of CO in the gaseous mixture decreases from 20.62% at 300 °C to 3.74% at 600 °C. The formation of CO is possibly due to the thermal decomposition of the carbonyl (C−O−C) and carboxyl (C═O) groups below 500 °C. At higher temperatures, it is due to lignin degradation. Figure 6 shows that the concentration of CH_4 increases from 4.10% at

https://doi.org/10.1021/acsomega.2c02076
ACS Omega 2022, 7, 28052−28064

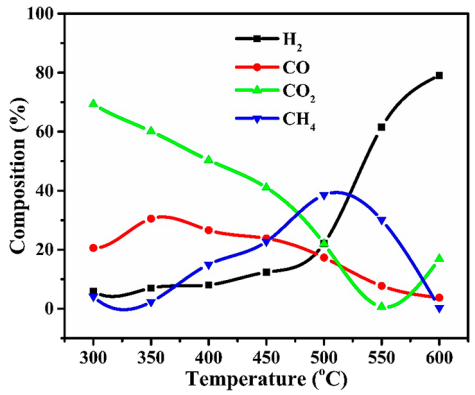

Figure 8. Effect of temperature on the composition of gaseous products.

300 °C to 38.55% at 500 °C and then decreases to 0.28% at 600 °C. The release of CH_4 is mainly due to the methoxy (O−CH_3). The percentage of H_2 continuously increases from 5.93% at 300 °C to 79.07% at 600 °C. The hydrogen release is primarily due to the cracking and decomposition of aromatic rings and methoxy groups of lignin.[32]

The HHV of pyrolytic gases was estimated using the formula developed by Guangul et al.[54] at different temperatures. The HHV of the gas mixture increased from 5007.20 kJ/Nm^3 at 300 °C to 20,876.85 kJ/Nm^3 at 550 °C then decreased to 10,721.29 kJ/Nm^3 at 600 °C. The high HHV can be attributed to the presence of methane and hydrogen in the pyrolysis gas. The reduction in HHV at higher temperatures is due to insignificant generation of methane.

4. FUTURE PROSPECTS AND FURTHER RESEARCH

The inferences drawn on the basis of the present study would be useful for scaling up the production of biochar, biogas, and bio-oil through the pyrolysis of sugarcane leaves and tops and other nonwoody biomass feedstocks. Use of larger biomass particles as the feedstock for pyrolysis would make the process energy-efficient and economical. Further, by optimizing the heating rate and temperature range, it would be possible to improve the yield of the desired product: biochar, biogas, or bio-oil. Through the use of the fractional condensation of bio-oil, it would be possible to separate aliphatic acid esters and phenolic compounds to obtain better value-added products. Use of suitable catalysts during pyrolysis would be helpful in improving the chemical composition and yield of various products. Data collected using pilot size continuous pyrolysis units would be helpful in designing and operating full size gasifiers and pyrolyzers for nonwoody biomass.

Chemical and thermal (torrefaction) pretreatment of biomass is likely to change the natural morphology and disrupt some of the natural bonds and would in turn lead to changes in the nature and quantity of pyrolysis products. This needs to be properly investigated and optimized.

The decentralized availability of the waste biomass from sugarcane fields poses a collection problem and makes it economically unattractive as a feedstock. To overcome this problem, it would be interesting to develop modular gasifiers and pyrolyzers that can be installed as close to the cane fields as possible. Briquetting and torrefaction of briquettes would minimize the handling, storage, and transportation problems. Hence, it would be interesting to prepare briquettes of the cane biomass and investigate its gasification and pyrolysis behavior with and without torrefaction. Efforts should also be made to study the co-pyrolysis of bagasse and sugar cane trash for assessing the possibility of maximum utilization of the waste biomass generated through cane cultivation and sugar manufacture.

Attempts are also made to improve the nature and yields of biochar, biogas, and bio-oil obtained from the pyrolysis of some biomasses using fast pyrolysis at extremely high heating rates, catalytic co-pyrolysis, and torrefaction and fractional condensation. Ratchahat et al.[55] have pyrolyzed cellulose in molten salt in the presence of a Ni catalyst supported on Al_2O_3. They have reported that the rapid heating rate (141 °C/s) provided by the molten salt system reduces the tar and CO_2 formation by 10-fold. The nickel catalyst helps in further reduction in tar formation by 5-fold due to the enhanced heating rate (181 °C/s). The catalyst deactivation is, however, a serious issue. Hakimian et al.[56] have carried out catalytic co-pyrolysis of waste oil sludge and microcrystalline cellulose powder (<20 μm) with the aim of increasing the yield of aromatics. Acidic zeolites of high microporosity have been used as catalysts, and Ni/HZSM-5 has been found to be the best catalyst. In view of the extremely complex nature of the co-pyrolysis process, use of ANN and machine learning has been recommended for process optimization. Selvarajoo et al.[57] have prepared biochar from citrus peel biomass using slow pyrolysis in the temperature range of 300 to 700 °C. They have observed that a higher yield of biochar is obtained at the lower pyrolysis temperature. The carbon and energy contents of biochar increase with increasing pyrolysis temperature, and the biochar produced at 500 °C having the highest HHV and carbon content is the best fuel. Valizadeh et al.[58] have evaluated the effects of temperature, torrefaction, and fractional condensation on the production of bio-oil from wood sawdust. It has been reported that the percentage of acids decreased from 17.29 to 12.76% on increasing the temperature from 300 to 600 °C and that of phenols increased from 31.03 to 37.37%. The fractional condensation results in reduction in the acidic components and increase in phenolics (up to 65.42%). It would be interesting to extend some of these studies on sugarcane trash, in particular, the overall economics and energy efficiency of the process.

5. CONCLUSIONS

The thermochemical characteristics and thermal degradation behavior of sugarcane leaves and tops have been investigated using powdered biomass. The batch pyrolysis experiments have been carried out using a fixed-bed tubular reactor. Effects of bed height (4−16 cm), particle size (0.180−0.710 mm), heating rate (15-30 °C/min), and temperature (350-650 °C) on yields of bio-oil, biogas and biochar have been investigated. The maximum yields of bio-oil (44.7%), biogas (36.67%), and biochar (36.82%) are obtained at 550, 650, and 350 °C, respectively, for a 16 cm deep bed of particles of size 0.18−0.30 mm at the heating rate of 25 °C/min. Several aliphatic, aromatic, phenolic, ketonic, and other acidic compounds are present in the bio-oil. It can be used as a fuel and feedstock for value-added products after appropriate refining and up-gradation. The biochar has a highly porous structure and several micronutrients, making it useful as a soil conditioner and adsorbent. In the middle temperature ranges, biogas had more methane and CO and less hydrogen, but at higher temperatures, hydrogen is the predominant constituent. The

https://doi.org/10.1021/acsomega.2c02076
ACS Omega 2022, 7, 28052−28064

economic viability and energy efficiency of the catalytic pyrolysis of biomass require further research.

■ ASSOCIATED CONTENT

Supporting Information

The Supporting Information is available free of charge at https://pubs.acs.org/doi/10.1021/acsomega.2c02076.

Particle size distribution and bulk density of powdered SCL biomass (Figure S1); FTIR spectra of bio-oil and biochar (Figure S2); and TGA and DTG curves of biochar at a heating rate of 15 °C/min (Figure S3) (PDF)

■ AUTHOR INFORMATION

Corresponding Author

Siddh Nath Upadhyay − *Department of Chemical Engineering &Technology, Indian Institute of Technology (Banaras Hindu University), Varana-si, Uttar Pradesh 221005, India;* orcid.org/0000-0003-2160-7584; Email: snupadhyay.che@itbhu.ac.in

Authors

Mohit Kumar − *Department of Chemical Engineering &Technology, Indian Institute of Technology (Banaras Hindu University), Varana-si, Uttar Pradesh 221005, India; Department of Sustainable Energy Engineering, Indian Institute of Technology, Kanpur, Uttar Pradesh 208016, India*

P. K. Mishra − *Department of Chemical Engineering &Technology, Indian Institute of Technology (Banaras Hindu University), Varana-si, Uttar Pradesh 221005, India*

Complete contact information is available at: https://pubs.acs.org/10.1021/acsomega.2c02076

Author Contributions

M.K. did a literature search, ran all the experiments, assessed the results, and wrote the first version of the manuscript. S.N.U. assisted in the design of the experiments, data analysis, and paper revision and oversaw the entire project. P.K.M. assisted in the design of the experiments, data analysis, and paper revision and oversaw the entire project.

Notes

The authors declare no competing financial interest.

■ ACKNOWLEDGMENTS

The authors are grateful to the Coordinator of the CIFC, IIT (BHU) Varanasi. The authors also acknowledge the Professor-in-Charge of AIRF, JNU, New Delhi, for giving permission to perform the GCMS analysis.

■ REFERENCES

(1) Xu, C.; Chen, Y.; Yang, H.; Chen, W.; Wang, X.; Chen, H. Fast pyrolysis of cotton stalk biomass using calcium oxide. *Bioresour. Technol.* **2017**, *233*, 5−20.

(2) Sindhu, R.; Gnansounou, E.; Binod, P.; Pandey, A. Bioconversion of sugarcane crop residue for value added products: An overview. *Renewable Energy* **2016**, *98*, 203−215.

(3) Charusiri, W.; Vitidsant, T. Upgrading bio-oil produced from the catalytic pyrolysis of sugarcane (*Saccharum officinarum* L) straw using calcined dolomite. *Sustainable Chem. Pharm.* **2017**, *6*, 114−123.

(4) Kumar, M.; Sabbarwal, S.; Mishra, P. K.; Upadhyay, S. N. Thermal degradation kinetics of sugarcane leaves (*Saccharum officinarum* L) using thermo-gravimetric and differential scanning calorimetric studies. *Bioresour. Technol.* **2019a**, *279*, 262−270.

(5) Nakashima, G. T.; Martins, M. P.; Hansted, A. L. S.; Yamamoto, H.; Yamaji, F. M. Sugarcane trash for energy purposes: Storage time and particle size can improve the quality of biomass for fuel. *Ind. Crops Prod.* **2017**, *108*, 641−648.

(6) Conag, A. T.; Villahermosa, J. E. R.; Cabatingan, L. K.; Go, A. W. Energy densification of sugarcane leaves through torrefaction under minimized oxidative atmosphere. *Energy Sustainable Dev.* **2018**, *42*, 160−169.

(7) Barros, J. A. S.; Krause, M. C.; Lazzari, E.; Bjerk, T. R.; do Amaral, A. L.; Caramão, E. B.; Krause, L. C. Chromatographic characterization of bio-oils from fast pyrolysis of sugar cane residues (straw and bagasse) from four genotypes of the Saccharum Complex. *Microchem. J.* **2018**, *137*, 30−36.

(8) da Cunha, M. E.; Schneider, J. K.; Brasil, M. C.; Cardoso, A. C.; Monteiro, L. R.; Mendes, F. L.; Pinho, A.; Jacques, R. A.; Machado, M. E.; Freitas, L. S.; Caramão, E. B. Analysis of fractions and bio-oil of sugar cane straw by one-dimensional and two-dimensional gas chromatography with quadrupole mass spectrometry (GC × GC/qMS). *Microchem. J.* **2013**, *110*, 113−119.

(9) Jutakridsada, P.; Sriprasoed, R.; Patikarnmonthon, N.; Kamwilaisak, K. Comparison study of sugarcane leaves and corn stover as a potential energy source in pyrolysis process. *Energy Procedia* **2016**, *100*, 26−29.

(10) Chen, Z.; Hu, M.; Zhu, X.; Guo, D.; Liu, S.; Hu, Z.; Xiao, B.; Wang, J.; Laghari, M. Characteristics and kinetic study on pyrolysis of five lignocellulosic biomass via thermogravimetric analysis. *Bioresour. Technol.* **2015**, *192*, 441−450.

(11) Río, C.; Lino, A. G.; Colodette, J. L.; Lima, C. F.; Martínez, T.; Lu, F.; Ralph, J.; Rencoret, J.; Guti, A. Biomass and Bioenergy Differences in the chemical structure of the lignins from sugarcane bagasse and straw. *Bioresour. Technol.* **2015**, *81*, 322−338.

(12) Charusiri, W.; Numcharoenpinij, N. Characterization of the optimal catalytic pyrolysis conditions for bio-oil production from brown salwood (*Acacia mangium Willd*) residues. *Biomass Bioenergy* **2017**, *106*, 127−136.

(13) Novais, S. V.; Zenero, M. D. O.; Tronto, J.; Conz, R. F.; Cerri, C. E. P. Poultry manure and sugarcane straw biochars modified with MgCl2 for phosphorus adsorption. *J. Environ. Manage.* **2018**, *214*, 36−44.

(14) Rueda-Ordóñez, Y. J.; Tannous, K. Isoconversional kinetic study of the thermal decomposition of sugarcane straw for thermal conversion processes. *Bioresour. Technol.* **2015**, *196*, 1−9.

(15) Kumar, M.; Upadhyay, S. N.; Mishra, P. K. A comparative study of thermochemical characteristics of lignocellulosic biomasses. *Bioresour. Technol. Rep.* **2019**, *8*, No. 100186.

(16) Mesa-Pérez, J. M.; Dilcio, J.; Barbosa-cortez, L. A.; Penedo-medina, M.; Alberto, C.; Cascarosa, E. Fast oxidative pyrolysis of sugar cane straw in a fluidized bed reactor. *Appl. Therm. Eng.* **2013**, *56*, 167−175.

(17) Moretti, M. M. D.; Perrone, O. M.; Nunes, C. D. C.; Taboga, S.; Boscolo, M.; da Silva, R.; Gomes, E. Effect of pretreatment and enzymatic hydrolysis on the physical-chemical composition and morphologic structure of sugarcane bagasse and sugarcane straw. *Bioresour. Technol.* **2016**, *219*, 773−777.

(18) Jeong, C. Y.; Dodla, S. K.; Wang, J. J. Fundamental and molecular composition characteristics of biochars produced from sugarcane and rice crop residues and by-products. *Chemosphere* **2016**, *142*, 4−13.

(19) da Silva Maciel, G. P.; Machado, M. E.; Barbara, J. A.; Molin, D. D.; Caramao, E. B.; Jacques, R. A. GC GC/TOFMS analysis concerning the identification of organic compounds extracted from the aqueous phase of sugarcane straw fast pyrolysis oil. *Biomass Bioenergy* **2016**, *85*, 198−206.

(20) American Petroleum Institute. *API Recommended Practice Standard Procedure for Field Testing Drilling Fluids*. Dallas, Texas: The Institute, 1984.

(21) Chen, Y.; Aanjaneya, K.; Atreya, A. A study to investigate pyrolysis of wood particles of various shapes and sizes. *Fire Saf. J.* **2017**, *91*, 820−827.
(22) Atreya, A.; Olszewski, P.; Chen, Y.; Baum, H. R. The effect of size, shape and pyrolysis conditions on the thermal decomposition of wood particles and firebrands. *Int. J. Heat Mass Transfer* **2017**, *107*, 319−328.
(23) Charusiria, W.; Vitidsant, T. Biofuel production via the pyrolysis of sugarcane (*Saccharum officinarum* L.) leaves: Characterization of the optimal conditions. *Sustainable Chem. Pharm.* **2018**, *10*, 71−78.
(24) Kumar, A.; Gupta, P.; Kumar, R. Modelling of pyrolysis of large wood particles. *Bioresour. Technol.* **2009**, *100*, 3134−3139.
(25) Edreis, E. M. A.; Luo, G.; Yao, H. Investigations of the structure and thermal kinetic analysis of sugarcane bagasse char during non-isothermal CO_2 gasification. *J. Anal. Appl. Pyrol.* **2014**, *107*, 107−115.
(26) Athira, G.; Bahurudeen, A.; Appar, S. Thermochemical Conversion of Sugarcane Bagasse: Composition, Reaction Kinetics, and Characterisation of By-Products. *Sugar Tech* **2021**, *23*, 433−452.
(27) Mishra, R. K.; Mohanty, K. Thermocatalytic conversion of non-edible Neem seeds towards clean fuel and chemicals. *J. Anal. Appl. Pyrolysis* **2018**, *134*, 83−92.
(28) Xiong, Z.; Wanga, Y.; Shatir, S.; Hassanc, S. A.; Hud, X.; Hana, H.; Sua, S.; Xua, K.; Long Jianga, L.; Guo, J.; Bertholdb, E. E. S.; Hua, S.; Xiang, J. Effects of heating rate on the evolution of bio-oil during its pyrolysis. *Energy Convers. Manage.* **2018**, *163*, 420−427.
(29) Luo, S.; Feng, Y. The production of hydrogen-rich gas by wet sludge pyrolysis using waste heat from blast-furnace slag. *Energy.* **2016**, *113*, 845−851.
(30) Oudenhoven, S. R. G.; Westerhof, R. J. M.; Kersten, S. R. A. Fast pyrolysis of organic acid leached wood, straw, hay and bagasse: improved oil and sugar yields. *J. Anal. Appl. Pyrolysis* **2015**, *116*, 253−262.
(31) Moralı, U.; Yavuzel, N.; Şensöz, S. Pyrolysis of hornbeam (*Carpinusbetulus* L.) sawdust: characterization of bio-oil and bio-char. *Bioresour. Technol.* **2016**, *21*, 682−685.
(32) Gupta, G. K.; Mondal, M. K. Experimental process parameters optimization and in-depth product characterizations for teak sawdust pyrolysis. *Waste Manage.* **2019**, *87*, 499−511.
(33) Zhang, H.; Xiao, R.; Huang, H.; Xiao, G. Comparison of non-catalytic and catalytic fast pyrolysis of corncob in a fluidized bed reactor. *Bioresour. Technol.* **2009**, *100*, 1428−1434.
(34) David, E.; Kopac, J. Pyrolysis of rapeseed oil cake in a fixed bed reactor to produce bio-oil. *J. Anal. Appl. Pyrolysis* **2018**, *134*, 495−502.
(35) Mante, O. D.; Agblevor, F. A.; Oyama, S. T.; McClung, R. The influence of recycling non-condensable gases in the fractional catalytic pyrolysis of biomass. *Bioresour. Technol.* **2012**, *111*, 482−490.
(36) Rout, T.; Pradhan, D.; Singh, R. K.; Kumari, N. Exhaustive study of products obtained from coconut shell pyrolysis. *J. Environ. Chem. Eng.* **2016**, *4*, 3696−3705.
(37) Capunitan, J. A.; Capareda, S. C. Assessing the potential for biofuel production of corn stover pyrolysis using a pressurized batch reactor. *Fuel* **2012**, *95*, 563−572.
(38) Demiral, I.; Kul, S. Ç. Pyrolysis of apricot kernel shell in a fixed-bed reactor: characterization of bio-oil and char. *J. Anal. Appl. Pyrolysis* **2014**, *107*, 17−24.
(39) Abnisa, F.; Arami-Niya, A.; Wan Daud, W. M. A.; Sahu, J. N.; Noor, I. M. Utilization of oil palm tree residues to produce bio-oil and bio-char via pyrolysis. *Energy Convers. Manage.* **2013**, *76*, 1073−1082.
(40) Biswas, B.; Pandey, N.; Bisht, Y.; Singh, R.; Kumar, J.; Bhaskar, T. Pyrolysis of agricultural biomass residues: Comparative study of corn cob, wheat straw, rice straw and rice husk. *Bioresour. Technol.* **2017**, *237*, 57−63.
(41) Mullen, C. A.; Strahan, G. D.; Boateng, A. A. Characterization of various fast-pyrolysis bio-oils by NMR spectroscopy. *Energy Fuels* **2009**, *23*, 2707−2718.
(42) Tag, A. T.; Duman, G.; Ucar, S.; Yanik, J. Effect of feedstock type and pyrolysis temperature on potential applications of biochar. *J. Anal. Appl. Pyrolysis* **2016**, *120*, 200−206.
(43) Anupam, K.; Sharma, A. K.; Lal, P. S.; Dutta, S.; Maity, S. Preparation, Characterization and optimization for upgrading *Leucaenaleucocephala*bark to biochar fuel with high energy yielding. *Energy* **2016**, *106*, 743−756.
(44) Wang, Z.; Cao, J.; Wang, J. Pyrolysis characteristics of pine wood in a slowly heating and gas sweeping fixed-bed reactor. *J. Anal. Appl. Pyrolysis* **2009**, *84*, 179−184.
(45) He, P.; Liu, Y.; Shao, L.; Zhang, H.; Lu, F. Particle size dependence of the physicochemical properties of biochar. *Chemosphere* **2018**, *212*, 385−392.
(46) Zhang, J.; Lu, F.; Zhang, H.; Shao, L.; Chen, D.; He, P. Multistage visualization of the structural and the characteristics changes of sewage sludge biochar oriented towards potential agronomic and environmental implications. *Sci. Rep.* **2015**, *5*, 9406.
(47) Yang, H.; Yan, R.; Chen, H.; Lee, D. H.; Zheng, C. Characteristics of hemicelluloses, cellulose and lignin pyrolysis. *Fuel* **2007**, *86*, 1781−1788.
(48) Angın, D. Effect of pyrolysis temperature and heating rate on biochar obtained from pyrolysis of safflower seed press cake. *Bioresour. Technol.* **2013**, *128*, 593−597.
(49) Balagurumurthy, B.; Srivastava, V.; Kumar, J.; Biswas, B.; Singh, R.; Gupta, P.; Kumar, K. S.; Singh, R.; Bhaskar, T. Value addition to rice straw through pyrolysis in hydrogen and nitrogen environments. *Bioresour. Technol.* **2015**, *188*, 273−279.
(50) Yakkala, K.; Yu, M. R.; Roh, H.; Yang, J. K.; Chang, Y. Y. Buffalo weed (*Ambrosia trifida L. var. trifida*) biochar for cadmium (II) and lead (II) adsorption in single and mixed system. *Desalin. Water Treat.* **2013**, *51*, 7732−7745.
(51) Mazlan, M. A. F.; Uemura, Y.; Osman, N. B.; Yusup, S. Characterizations of Bio-char from Fast Pyrolysis of Meranti Wood Sawdust. *J. Phys.: Conf. Ser.* **2015**, *622*, No. 012054.
(52) Salgado, M. D. F.; Abioye, A. M.; Junoh, M. M.; Antos, J. A. P.; Ani, F. N. Preparation of activated carbon from *babassuendocarpunder* microwave radiation by physical activation. *IOP Conf. Series: Earth and Environmental Science*. 2017, *105*, 012116.
(53) Jahirul, M. I.; Rasul, M. G.; Chowdhury, A. A.; Ashwath, N. Biofuels production through biomass pyrolysis − A technological review. *Energies* **2012**, *5*, 4952−5001.
(54) Guangul, F. M.; Sulaiman, S. A.; Ramli, A. Study of the effects of operating factors on the resulting producer gas of oil palm fronds gasification with a single throat downdraft gasifier. *Renewable Energy* **2014**, *72*, 271−283.
(55) Ratchahat, S.; Srifa, A.; Koo-amornpattana, W.; Sakdaronnarong, C.; Charinpanitkul, T.; Wu, K. C. W.; Show, P. L.; Kodama, S.; Tanthapanichakoon, W.; Sekiguchi, H. Syngas production with low tar content from cellulose pyrolysis in molten salt combined with Ni/Al_2O_3 catalyst. *J. Anal. Appl. Pyrolysis* **2021**, *158*, 105243.
(56) Hakimian, H.; Pyo, S.; Kim, Y. M.; Jae, J.; Show, P. L.; Rhee, G. H.; Chen, W. H.; Park, Y. K. Increased aromatics production by co-feeding waste oil sludge to the catalytic pyrolysis of cellulose. *Energy* **2022**, *239*, 122331.
(57) Selvarajoo, A.; Wong, Y. L.; Khoo, K. S.; Chen, W. H.; Show, P. L. Biochar production via pyrolysis of citrus peel fruit waste as a potential usage as solid biofuel. *Chemosphere* **2022**, *294*, No. 133671.
(58) Valizadeh, S.; Oh, D.; Jae, J.; Pyo, S.; Jang, H.; Yim, H.; Rhee, G. H.; Khan, M. A.; Jeon, B. H.; Lin, K. Y. A.; Show, P. L.; Sohn, J. M.; Park, Y. K. Effect of torrefaction and fractional condensation on the quality of bio-oil from biomass pyrolysis for fuel applications. *Fuel* **2022**, *312*, No. 122959.

https://doi.org/10.1021/acsomega.2c02076
ACS Omega 2022, 7, 28052−28064